Environmental Science & Technology

Article

pubs.acs.org/est

Atmospheric Evolution of Sulfur Emissions from Kīlauea: Real-Time Measurements of Oxidation, Dilution, and Neutralization within a Volcanic Plume

Jesse H. Kroll,*[,†,#] Eben S. Cross,[†,#] James F. Hunter,[†] Sidhant Pai,[†] TREX XII,[∥] TREX XI,[¶] Lisa M. M. Wallace,[‡] Philip L. Croteau,[§] John T. Jayne,[§] Douglas R. Worsnop,[§] Colette L. Heald,[†] Jennifer G. Murphy,[⊥] and Sheila L. Frankel[†]

[†]Department of Civil and Environmental Engineering, Massachusetts Institute of Technology, Cambridge, Massachusetts, United States

[§]Center for Aerosol and Cloud Chemistry, Aerodyne Research, Inc., Billerica, Massachusetts, United States

[‡]Air Surveillance and Analysis Section, Hawai'i State Department of Health, Hilo, Hawai'i, United States

[⊥]Department of Chemistry, University of Toronto, Toronto, Ontario, Canada

Supporting Information

ABSTRACT: The high atmospheric concentrations of toxic gases, particulate matter, and acids in the areas immediately surrounding volcanoes can have negative impacts on human and ecological health. To better understand the atmospheric fate of volcanogenic emissions in the near field (in the first few hours after emission), we have carried out real-time measurements of key chemical components of the volcanic plume from Kīlauea on the Island of Hawai'i. Measurements were made at two locations, one ∼3 km north-northeast of the vent and the other 31 km to the southwest, with sampling at each site spanning a range of meteorological conditions and volcanic influence. Instrumentation included a sulfur dioxide monitor and an Aerosol Chemical Speciation Monitor, allowing for a measurement of the partitioning between the two major sulfur species (gas-phase SO_2 and particulate sulfate) every 5 min. During trade wind conditions, which sent the plume toward the southwest site, sulfur partitioning exhibited a clear diurnal pattern, indicating photochemical oxidation of SO_2 to sulfate; this enabled the quantitative determination of plume age (5 h) and instantaneous SO_2 oxidation rate (2.4×10^{-6} s^{-1} at solar noon). Under stagnant conditions near the crater, the extent of SO_2 oxidation was substantially higher, suggesting faster oxidation. The particles within the plume were extremely acidic, with pH values (controlled largely by ambient relative humidity) as low as −0.8 and strong acidity (controlled largely by absolute sulfate levels) up to 2200 nmol/m^3. The high variability of sulfur partitioning and particle composition underscores the chemically dynamic nature of volcanic plumes, which may have important implications for human and ecological health.

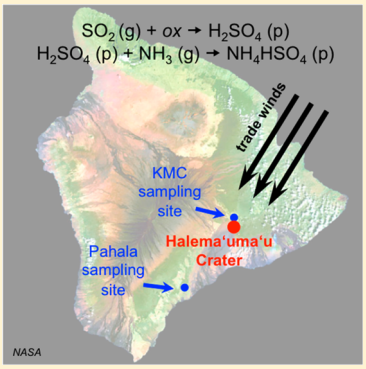

INTRODUCTION

Volcanoes are a major source of sulfur to the atmosphere, accounting for ∼20−40% of natural sulfur emissions and ∼10% of sulfur emissions overall.[1] Gaseous forms of volcanogenic sulfur include sulfur dioxide (SO_2, 13.4 Tg/yr), hydrogen sulfide (H_2S, 2.8 Tg/yr), and other trace species.[2] Particulate sulfate (SO_4^{2-}) is also emitted directly from volcanoes,[3] although most volcanogenic sulfate is secondary, formed from the atmospheric oxidation of SO_2. Because of the large impact that sulfate particles have on the radiative balance of the atmosphere, via direct interactions with radiation as well as modification of cloud properties and lifetimes,[4] much of the focus on volcanoes in the atmospheric chemistry literature has been on quantifying their impact on past and present climate. However, volcanic emissions can also have adverse impacts on human and ecological health. It is estimated that over 450 million people worldwide live near active volcanoes,[5] and toxic volcanic gases and particulate matter therefore are likely to pose a health hazard globally.[6,7]

Within the United States, the dominant source of volcanic sulfur emissions is Kīlauea Volcano on the Island of Hawai'i. Kīlauea currently emits ∼1 Tg SO_2 per year;[8] this is smaller than anthropogenic SO_2 emissions in the U.S. (∼6 Tg SO_2/yr[9]) but derives from a single point source, and so can have major impacts on local health and ecology. The plume of volcanic emissions ("volcanic smog", or "vog") is known in the area as a major nuisance, and has been shown to have adverse cardiorespiratory health impacts on island residents.[10−13] This has been especially pronounced since March 2008, when a new

Received: December 16, 2014
Revised: February 23, 2015
Accepted: March 3, 2015
Published: March 3, 2015

DOI: 10.1021/es506119x
Environ. Sci. Technol. 2015, 49, 4129−4137

vent opened in the Halema'uma'u crater (see Supporting Information (SI) Figure S1), shifting the majority of the volcano's emissions further inland, increasing the vog exposure of local residents, and leading to exacerbated health effects.[14,15] Because the meteorology is dominated by strong trade winds, most of the time the Halema'uma'u plume travels to the southwest, passing through communities such as Pahala (population 1356). Communities on the west coast (such as Kailua, population 11 975) can also be affected via onshore/offshore winds. However, at times (especially in the winter), the wind pattern can reverse, with "Kona winds" sending the plume to the northeast, toward more populous areas such as Hilo (population 43 263). Thus, the Halema'uma'u plume has the potential to affect the health and well-being of a large number of people living in the region.

The detailed impact of such volcanic emissions on human and ecological health is a function of not only the plume's intensity (which is controlled by emission rate and transport) but also the relative abundance of various chemical species within the plume. Because of chemical reactions that take place within the plume, the plume composition is highly dynamic[16,17] and dependent on a number of factors that vary with time and location (e.g., meteorological conditions, sunlight, and local emissions). Such reactions will govern the amount and composition of volcano-derived particulate matter; key reactions are the oxidation of SO_2 to form particulate sulfuric acid,[18] and the subsequent neutralization of the sulfuric acid by ambient ammonia to form ammonium sulfate salts:[19,20]

$$SO_2(g) + ox \rightarrow H_2SO_4(p) \quad (R1)$$

$$H_2SO_4(p) + NH_3(g) \rightarrow NH_4HSO_4(p) \quad (R2)$$

$$NH_4HSO_4(p) + NH_3(g) \rightarrow (NH_4)_2SO_4(p) \quad (R3)$$

where "g" and "p" denote the gas phase and particle phase, respectively, and "ox" refers to oxidant (in the gas or condensed phase). Because the loadings and composition of the particles are likely to play a role in the human and ecological effects of the plume, it is important that the details and rates of these reactions be well understood. However, although substantial effort has gone into understanding the emissions, and chemistry of volcanic SO_2 (as well as trace volcanic species, such as H_2S, HCl, etc.),[16,17,21−24] the detailed chemistry underlying the formation and evolution of volcano-derived particulate matter has received less study. This is in part due to the challenges associated with measuring particle composition. Mass measurements of $PM_{2.5}$ (particulate matter of diameter 2.5 μm or smaller) are of limited utility for constraining volcanic emissions because of the contribution from non-volcanogenic sources of aerosol, such as fossil fuel burning and dust. Particle composition can be determined from filter-based collection, followed by offline chemical analysis,[3,19,20,24,25] but because sample collection typically requires a few hours to days per filter, such measurements suffer from poor time resolution, providing limited information on temporal variability. Such techniques are also subject to sampling or chemical artifacts, such as from neutralization of acidic sulfate.

In this study, we apply a relatively new technique, aerosol mass spectrometry,[26,27] to the characterization of the evolving chemistry of the Kīlauea plume during the first several hours after emission. The high time resolution (a few minutes per measurement) of this technique allows for the characterization of rapid changes in plume chemistry. Volcanic plumes have previously been detected using aerosol mass spectrometry;[28−31] however, this study represents the first use of the technique in the near-field, aimed at characterizing the temporal variability in particle composition that arises from sulfur oxidation and neutralization reactions. Measurements were made at two different sites, under varying meteorological conditions and plume ages, providing insight into the factors controlling the mass and chemical composition of volcano-derived sulfate particles.

MATERIALS AND METHODS

All measurements were made on the Island of Hawai'i in January−February 2013 as part of TREX ("Traveling Research Environmental eXperience"), an MIT undergraduate class covering fieldwork in environmental science and engineering. Emissions from the vent of Kīlauea's Haleama'uma'u crater were sampled at two locations over the course of the study (see SI, Figure S1). From January 17 to January 23, measurements were made at Kilauea Military Camp (KMC), located on the north rim of the crater, ∼3 km north-northeast of the vent. For these measurements, the instruments were housed inside a minivan, which enabled mobile measurements (not discussed here). Subsequent measurements (January 23 to February 6) were made in the town of Pahala, located 31 km southwest (directly downwind during typical synoptic flow) of the vent. These measurements were taken within the Hawai'i Department of Health (DOH) air quality monitoring station located in the town.

The key chemical measurements were of fine particles (mass concentration and chemical composition) and sulfur dioxide, allowing for the detailed characterization of major sulfur-containing species (sulfate and SO_2) with high (∼5 min) time resolution. Particle mass and composition were measured in real time using an Aerodyne Aerosol Chemical Speciation Monitor (ACSM). The design and operation of this instrument is described in detail elsewhere.[27] Briefly, sampled particles are aerodynamically focused into the high-vacuum detection region, where they are thermally vaporized at 600 °C and analyzed using electron impact mass spectrometry. The resulting aerosol mass spectra provide online real-time mass concentrations of nonrefractory aerosol species (sulfate, nitrate, ammonium, chloride, and organics). The ACSM detects particles with vacuum aerodynamic diameters of 75−650 nm, which spans nearly the entire accumulation mode, so that all secondary sulfate is likely to be measured. However, primary volcanic particles can be somewhat larger than this, with ∼50% of the sulfate mass found in particles larger than 650 nm.[20,25] This might imply that primary sulfate is somewhat underestimated in the present study, although this effect is difficult to quantify because of the lack of sizing measurements and the unknown role that particulate water plays in controlling particle size. Background sulfate levels (a combination of background ambient levels plus instrumental background) were 0.18 and 0.075 $\mu g/m^3$ at KMC and Pahala, respectively, as determined from measurements during clean periods; these values were subtracted from all measurements to isolate concentrations of volcanic sulfate. At KMC, air was sampled through a 1.5 m section of a 1/4-in.-o.d. copper inlet at 1.5 SLPM, positioned out the rear passenger window of the minivan. At Pahala, the PM inlet system was extended (3.7 m total length) to colocate the sampling inlet with that of the DOH instrumentation. A Nafion drier was used to control the relative humidity (30−55%) of the sampled air. Filtered ambient air from a sampling

DOI: 10.1021/es506119x
Environ. Sci. Technol. 2015, 49, 4129−4137

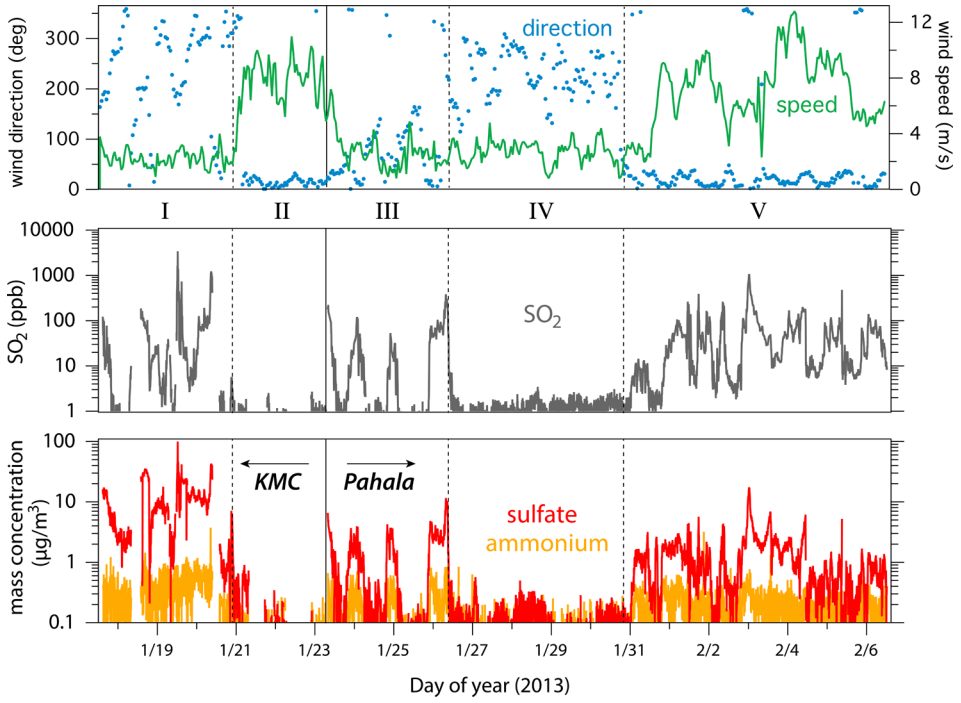

Figure 1. Summary of meteorological parameters and plume composition measurements. Top panel: wind direction (0°/360° refers to wind from due north) and wind speed, measured at HVO near the crater, showing five distinct meteorological conditions during sampling (I and IV, relatively stagnant; II and V, trade winds; III, transitional). Sampling was at KMC (near the crater) during periods I and II and at Pahala (31 km to the southwest) during periods III–V. Middle panel: SO_2 concentrations. Bottom panel: mass concentrations of particulate sulfate and ammonium, as measured by the ACSM.

pump (KNF) was used to provide the drier with continuous sheath flow. The temperature and relative humidity of the PM inlet air were monitored and logged throughout the campaign. For all measurements, a collection efficiency of 1 was used, based on the highly acidic nature of the particles.[32] Other details of the operation and calibration of the ACSM are given in the Supporting Information. Measurements were made every 4.8 min.

SO_2 measurements were made using a UV fluorescence monitor (Teledyne 100E), with ambient air sampled via a 1/4-in.-o.d. Teflon line colocated with the PM sampling inlet. The instrument was calibrated at the Pahala DOH station with ambient SO_2, using the measurements from the regularly calibrated DOH monitor (Thermo Model 43C). Signals from both instruments, spanning several orders of magnitude in SO_2 concentration, were highly correlated (R^2 = 0.997), enabling this in-field calibration. All measurements required a zero-offset correction, which was determined from measurements of air free of volcanic influence, and found to be different at Pahala (1.9 ppb) from at KMC (14.9 ppb). The reason for this difference is not clear, but may be related to the elevation difference (292 vs 1220 m) at the two sites. SO_2 measurements were made every minute, although for comparison with aerosol data, they were averaged over the 2.4 min time periods during which the ACSM was sampling ambient air.

Other ancillary measurements include local temperature and relative humidity (Sensirion, 1 s time resolution), used for calculations of aerosol pH. Wind speed, wind direction, and other meteorological parameters were also measured at the Pahala DOH station, but these were heavily influenced by local meteorology, specifically upslope/downslope flow (SI Figure S2), and thus provide limited insight into the overall trajectory of the volcanic plume. Instead, wind speed and wind direction are taken from the hourly measurements made by the National Park Service (available at http://ard-request.air-resource.com/), taken at the USGS Hawaiian Volcano Observatory (HVO). The HVO is located on a flat plain on the northwest rim of the crater, and hence, such measurements provide information on the overall meteorology at a given time (e.g., trade wind conditions vs stagnant conditions) and, thus, on the transport of the volcanic plume just after emission.

RESULTS AND DISCUSSION

Meteorological Conditions. Key measurements of the meteorology and sulfur chemistry taken over the course of the entire study (wind speed and direction, [SO_2], and sulfate and ammonium loading) are shown in Figure 1. (All dates and times are local, UTC−10:00.) The meteorological measurements (top panel) indicate that there were five distinct periods during sampling. Two of the periods (period I, Jan. 17–20; period IV, Jan. 26–30) were characterized by relatively stagnant conditions, with wind speeds between 0 and 4 m/s. Two others (II, Jan. 21–23; V, Jan. 31–Feb. 6) were characterized by trade winds, with winds coming from the north-northeast at speeds of 4–12 m/s. Period III (Jan. 23–26) was a transition between trade winds and stagnant conditions, involving generally weak, northerly winds. The instruments were moved from KMC to Pahala near the beginning of period III, so both stagnant and trade wind conditions were accessed at each sampling site. However, the two sites experience very different degrees of volcanic influence for a given meteorological condition because of differences in the positions of the two sites relative to the vent. During stagnant periods, volcanic emissions affect KMC but not Pahala, whereas trade winds send the emissions directly toward Pahala, leaving the air at KMC essentially free of direct volcanic influence. Thus, the periods in which volcanic

DOI: 10.1021/es506119x
Environ. Sci. Technol. 2015, 49, 4129–4137

influence is expected to be observed are period I (stagnant air, sampling at KMC) and period V (trade winds, sampling at Pahala) and, to a lesser extent, period III (weak northerly winds, sampling at Pahala). Measured SO_2 and sulfate levels (bottom two panels) are indeed highest during these periods, indicating that this simple description of the meteorology provides insight into the fate and transport of the volcanic plume.

SO_2, Sulfate, and Sulfur Partitioning. Measured SO_2 levels (Figure 1, middle panel) varied over an extremely wide range, from below 1 ppb (for times with no volcanic influence, periods II and IV) to over 3 ppm (stagnant conditions at KMC). Exceedingly high levels (>1 ppm) are also measured during times of trade wind influence in Pahala. Such high concentrations more than 30 km downwind of the source indicate the sustained intensity of the volcanic plume even after substantial advection. These high SO_2 levels are not unusual for Pahala, since trade wind conditions persist throughout the year, especially in nonwinter months (see SI Figure S3).

Particulate sulfate levels (Figure 1, bottom panel) were also high (up to ~100 $\mu g/m^3$) during periods of volcanic influence. Ammonium levels were generally measurable but small (usually <1 $\mu g/m^3$), indicating relatively little neutralization of the sulfate aerosol. The role of neutralization and aerosol acidity will be discussed below. Other particulate species measured by the ACSM (not shown) were minor; the one exception is organic aerosol, which occasionally spiked at KMC as a result of local wood-burning emissions, but this had no apparent influence on sulfate measurements. Measured chloride levels were negligible, consistent with recent work finding low Cl emissions from Kīlauea relative to other volcanoes.[24]

Although SO_2 and sulfate tend to co-vary (i.e., both are high during periods of volcanic influence), the overall correlation between the two species is relatively poor (R^2 = 0.37; see SI, Figure S4), indicating large variability in the extent of sulfur fractionation over the course of the study. Figure 2 shows how the partitioning of sulfur between the two species varied over the course of the study. Partitioning is expressed in terms of the fraction f_S of total sulfur in the form of particulate sulfate, given by $f_S = [SO_4^{2-}]/([SO_4^{2-}] + [SO_2])$, with all concentrations in molar units.[33] This calculation assumes that all sulfate is measured by the ACSM; if some fraction is not (e.g., some of the sulfate is present in particles outside the ACSM's size window), then the derived f_S value will be somewhat of an underestimate. For periods in which volcanic influence was minimal (II and IV), partitioning is likely controlled by non-volcanogenic sources of sulfur and is subject to considerable uncertainty, given the low concentrations of both species. The volcano-influenced periods (I, III, V) exhibit substantial variability in sulfur partitioning. Although differences in relative deposition rates may contribute to this variability, the main source is likely differences in photochemical age, the extent of oxidative processing between emission, and measurement. Under low-wind conditions, the SO_2 emissions can accumulate and over time convert to sulfate, leading to the large values of f_S in periods I and III. By contrast, under trade wind conditions (period V), the volcanic plume intercepted at Pahala was no more than a few hours old, with little time for SO_2-to-sulfate conversion, leading to much lower values of f_S. The relatively high value of f_S on Jan. 31 may have resulted from the onset of the trade winds, leading to advection of relatively aged emissions from the crater to Pahala.

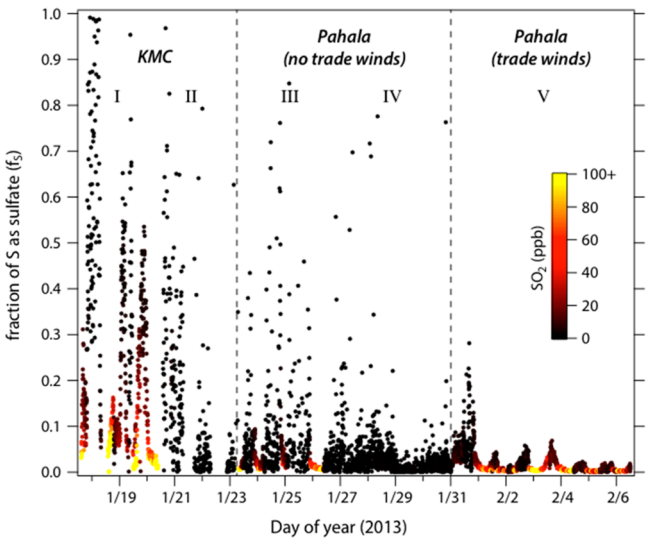

Figure 2. Measured sulfur partitioning (f_S) over the course of the study. Points are colored by SO_2 concentration. For times influenced by volcanic emissions, it is highest when the winds are lowest (periods I and III). During trade wind conditions, there is a clear diurnal pattern in f_S downwind of the crater (period V).

SO_2 oxidation kinetics. Period V (trade wind conditions, sampling at Pahala) is characterized by a clear diurnal cycle in sulfur partitioning, with f_S lowest at night and highest in the afternoon. Dry deposition might lead to changes in f_S due to differences in deposition rates of SO_2 and sulfate.[34] However, such differences are highly unlikely to exhibit the observed diurnal profile in f_S, which changes by up to a factor of 8 over the course of the day. Instead, this time-of-day dependence strongly suggests that the SO_2-to-sulfate conversion is driven by photochemical oxidation. Such oxidation is likely due to reaction with short-lived oxidants. Oxidation catalyzed by transition metal ions[35] is unlikely to be important, given that oxidation is primarily observed during the daytime only. Similarly, oxidation by aqueous O_3 is expected to be negligible because of the high acidity of the particles. Oxidation by Criegee intermediates[36] is also unlikely, given the presumably low concentrations of VOCs in the plume. Thus, the dominant oxidants are likely to be photolytically generated species, such as gas-phase OH or aqueous H_2O_2.

The evolving sulfur partitioning for a single day (Feb. 3) is shown in greater detail in Figure 3, along with that day's solar elevation angle (SEA). Before sunrise, both SO_2 and sulfate are at their highest levels of the day (likely due in part to the shallow boundary layer), but the sulfate fraction is at a minimum. At sunrise, the sulfate fraction starts increasing, reaching a peak of several percent in the afternoon before falling back to almost the previous night's value. This time dependence is similar during other days in period V, although with lower peak values of f_S (Figure 2).

Figure 3 shows a considerable lag between solar irradiation (which peaks at solar noon, 12:35 pm) and the peak in measured fractional sulfur conversion (which peaks at ~3:00 pm); elevated sulfate fractions are observed well after sunset. This time lag arises at least in part from the time elapsed between emission and sampling because the conversion of SO_2 to sulfate is governed by exposure to oxidants, which varies dramatically over the course of the day.

DOI: 10.1021/es506119x
Environ. Sci. Technol. 2015, 49, 4129−4137

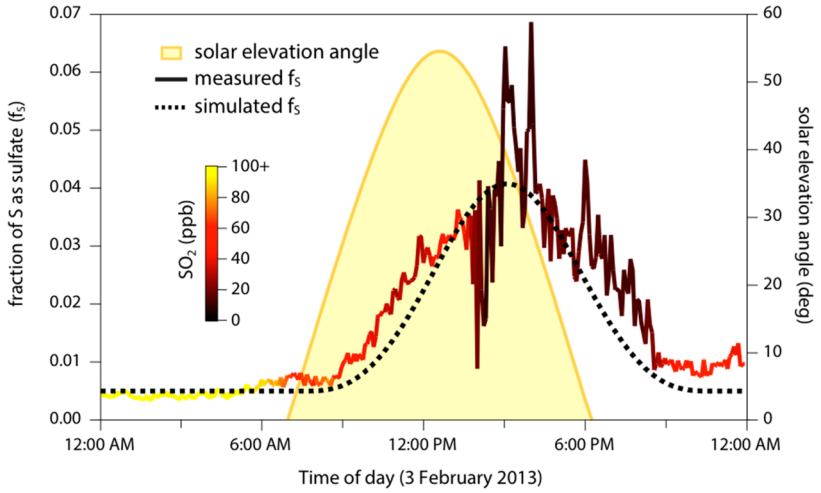

Figure 3. Evolving sulfur partitioning (f_S) at Pahala on Feb. 3, 2013 (a day characterized by trade winds). The diurnal profile in f_S (thick trace) indicates sunlight-initiated SO_2 oxidation to sulfate. Partitioning lags behind solar elevation angle (a metric of irradiation, shown in yellow), due to the transport time from the source to the sampling site. The dashed line denotes calculated f_S from a simple kinetic model matched to the observations; this enables estimates of the primary sulfate fraction (0.005), age of the plume (~5 h), and instantaneous SO_2 oxidation rate (2.4×10^6 s^{-1} at solar noon).

To better quantify this oxidation process, a simple kinetic model was constructed to relate transit time, SO_2 oxidation rate, and fractional sulfur conversion. First, some fraction of the sulfur is assumed to be primary (directly emitted from the volcano). This fraction, taken from the zero-offset in Figure 3, is ~0.005, consistent with previous measurements of primary sulfate emissions (on the order of 0.1−1% of total sulfur[3,20,37,38]); however, errors in the present value may arise from the size cutoff of the ACSM, or the potential contribution of secondary production of sulfate via nighttime oxidation of SO_2. Oxidation (the increase in f_S) is then simulated by assuming that the instantaneous oxidation rate is proportional to the ozone photolysis rate constant $J(O^1D)$ (i.e., that oxidation is driven by OH, or another oxidant with a similar diurnal profile). The time-of-day dependence of $J(O^1D)$ is estimated from SEA using the parametrization used in the Master Chemical Mechanism;[39] cloud cover was minimal on this day. Since oxidation occurs continually over the time between emission and sampling, the model integrates $J(O^1D)$ over some fixed transit time; this time is determined by adjusting it to match the peak in f_S. We note that if the observed time lag derives not only from the transport time but also from oxidant levels peaking later in the day (which would require the oxidants to be substantially longer-lived than OH), the transport time estimated using this approach would represent an upper limit. Finally, the instantaneous (time-dependent) SO_2 oxidation rate (s^{-1}) is determined from this transit time by adjusting the proportionality constant that relates $J(O^1D)$ to oxidation rate until the integrated amount of oxidation matches the observed f_S values (height of the paraboloid in Figure 3). Dry deposition is not explicitly included in the model; it is a highly uncertain process which, as discussed above, might affect f_S but likely not with the diurnal dependence observed.

Model results are shown as the dashed line in Figure 3; with the exception of the slightly narrower peak in simulated f_S (discussed below), the model reproduces the time-dependent f_S measurements well. Interestingly, the peak in the observed sulfate fraction can be reproduced only by assuming a 5 h transit time, substantially longer than what would be expected on the basis of wind speed and distance alone (~1.1 h). As noted above, this inferred transit time may be somewhat of an overestimate if sulfate formation is driven by long-lived oxidants that peak late in the day. Nonetheless, this result suggests that the plume was not transported directly to Pahala, but instead was influenced by local topographic and meteorological factors, a conclusion that is strongly supported by measured differences in local winds at the crater and Pahala (SI Figure S2). During these trade wind days (period V, 1/31/13−2/7/13), winds at the crater were mostly from the north-northeast, with an average speed of 6.8 m/s, whereas at Pahala, the winds were predominantly from the east/southeast (in the morning) or northwest (in the afternoon and night), with an average speed of only 2.0 m/s. Thus, even on trade wind days, the volcanic plume did not take a direct path from the crater to Pahala, but rather reached Pahala via upslope/downslope flow. This longer transit distance and slower wind speed implies a substantially longer transit time than would be expected based on the simple (and commonly used) calculation based on wind speed and distance, in agreement with our observations. SI Figure S2 also indicates that the transit time likely varies over the course of the day; this may explain why our simple model does not fully capture the observed time-dependence of the oxidation (somewhat underestimating the width of the paraboloid in Figure 3).

The model also provides an estimate of the time-dependent SO_2 oxidation rate. The maximum (noontime) oxidation rate is 2.4×10^{-6} s^{-1}, and the 24-h average oxidation rate is 5.3×10^{-7} s^{-1}, yielding an SO_2 lifetime vs oxidation under these conditions of ~22 days. To our knowledge, this represents the first diurnally resolved measurement of the instantaneous SO_2 oxidation rate within a volcanic plume. Assuming the oxidation is by gas-phase OH (and using $k_{OH+SO_2} = 8.9 \times 10^{-13}$ cm^3 $molecule^{-1}$ s^{-1}),[40] these observed rates correspond to an equivalent peak [OH] of 2.7×10^6 molecules cm^{-3}, and an equivalent diurnally averaged [OH] of 5.9×10^5 molecules cm^{-3}. Such concentrations are lower than typical ambient values of [OH] for the tropics,[41] suggesting suppression of OH within the plume, presumably due to the very high SO_2 concentrations.

DOI: 10.1021/es506119x
Environ. Sci. Technol. 2015, 49, 4129−4137

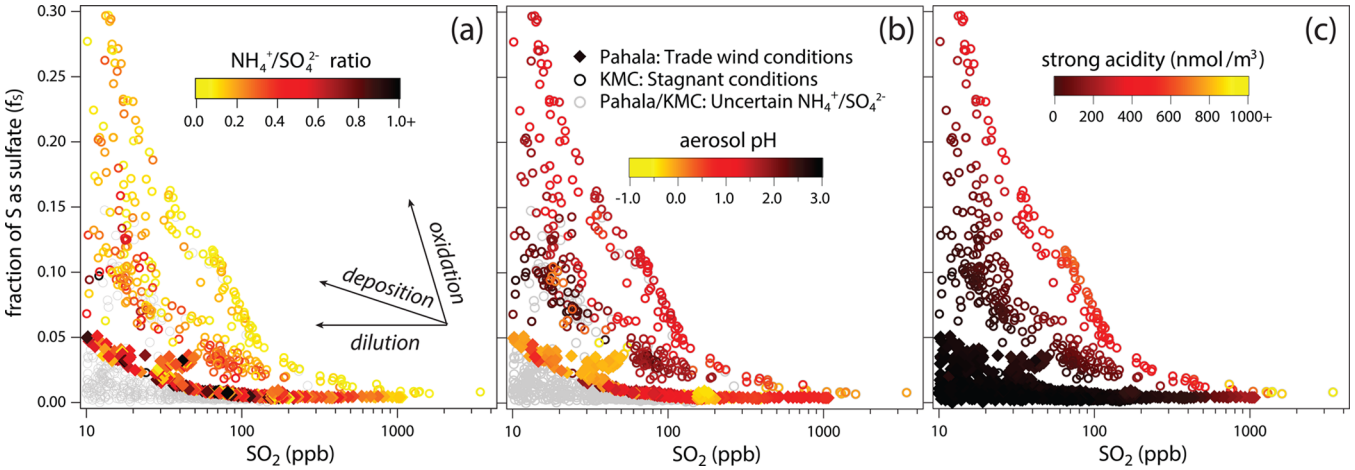

Figure 4. Changes to volcanic emissions due to dilution, deposition, oxidation, and neutralization. Measurements from periods I (KMC, stagnant) and V (Pahala, trade winds) are shown, plotted as f_S (sulfur partitioning) vs $[SO_2]$ (a rough measure of plume dispersion since emission). Movement in this space corresponds to different processes affecting sulfate levels (dilution, deposition, and oxidation), as shown by the arrows in panel a. Marker color denotes degree of neutralization, with yellow denoting the most acidic particles, using three different acidity metrics. Panel a: ammonium/sulfate ratio. Panel b: aerosol pH. Panel c: strong acidity.

The measured rate of SO_2 oxidation (5.3×10^{-7} s^{-1}) is on the low end of previous estimates of SO_2 loss rates within tropospheric volcanic plumes, which range from 2×10^{-7} s^{-1} to $\sim 10^{-4}$ s^{-1}.[8,18,20,25,28,33,42−48] (Some near-field measurements[49] found even faster rates of loss ($>10^{-3}$ s^{-1}), although those measurements may have been biased high as a result of variations in emissions.[18]) In fact, on subsequent trade wind days (Feb. 4−6) the estimated oxidation rate is lower still (by a factor of 2−3), making our measurements of SO_2 oxidation rate among the lowest ever reported. Focusing on Kīlauea only, two previous studies (one ground-based[45] and one satellite-based[8]) of SO_2 from Kīlauea found the conversion time to be 5.8×10^{-6} to 1.2×10^{-5} s^{-1} and 3.2×10^{-5} s^{-1}, respectively, both significantly faster than the rate determined here. Even if the transit time is shorter than the inferred value of 5 h and, instead, is closer to the lower-limit value of 1.1 h (which, as discussed above, is likely an underestimate), the inferred oxidation rates would increase by only a factor of 4.5, and thus are still lower than most previous measurements.

Part of the reason for the differences between determined rates may be methodological. In the present study, both SO_2 and sulfate are measured directly, and primary sulfate is explicitly accounted for; in studies in which sulfate is not directly measured but rather inferred, calculated rates can be influenced (mostly overestimated) by losses of SO_2 via nonoxidative processes (dilution, deposition), the presence of nonsulfate components of aerosol (e.g., water, ash, ammonium), and the importance of primary volcanic sulfate. In addition, because the present approach is based on fractional sulfur conversion, it does not assume that SO_2 emissions are fixed because that assumption can also complicate determinations of conversion rates.[18] Most importantly, the use of solar irradiation for determining the age of the sampled emissions is a unique feature of the present analysis. Most previous studies instead estimate age from average wind speed and distance; in areas with complex terrain and local meteorology, such as that of the present study, this approach can underestimate plume age, which would also lead to an overestimate in oxidation rate.

Despite the above considerations, the differences in inferred reactivities in the present study and in previous work may reflect real differences in plume composition and ambient oxidative conditions, leading to substantial variability in SO_2 oxidation rate. Our measurements were made in the wintertime, which (even in the tropics) is characterized by lower photochemical activity than in summer months.[41] The previous measurements of SO_2 oxidation within the Kīlauea plume were made in August[45] and March−November,[8] which may help explain the higher rates inferred in those studies. In addition, the plumes sampled in the present work were very well-defined, with sustained high SO_2 concentrations that would drive down oxidant levels. By contrast, less-concentrated plumes may be significantly more photochemically active, leading to SO_2 oxidation rates that would be substantially higher than the ones determined here.

For the earlier, non-trade-wind periods, the above approach for estimating plume age and SO_2 oxidation rate cannot be applied because of the lack of rapid, stable transport of emissions from the vent to the sampling site. The air sampled was therefore made up of emissions that span a wide range of atmospheric ages. Such a system is not easily analyzed using simple kinetics, especially given the lack of measurements that could help constrain the time of emission. Instead, we use $[SO_2]$ as a qualitative metric for the average plume age, since it provides information about the amount of dispersion that has taken place since emission (assuming emissions remain roughly constant).

Shown in Figure 4 are plots of f_S vs $[SO_2]$ for times of major volcanic influence (periods I and V). Only data with $[SO_2] \geq 10$ ppb are shown, to avoid errors associated with background concentrations and instrument zeroes. The coloring within the different panels is related to particle acidity, described below. The sulfur in fresh volcanic emissions is highly concentrated and present mostly in the form of $[SO_2]$. The average value of f_S for these fresh emissions (lower right corner of Figure 4), which corresponds to the fraction of sulfur emitted as primary volcanic sulfate, is ~0.008. This is slightly higher than the value inferred downwind (Figure 3), although again, this may be an underestimate, given the size cutoff of the ACSM. Dispersion of the emissions (dilution) leads to leftward movement in Figure 4 because SO_2 and sulfate are affected essentially equally. (Some changes to f_S may occur in the most dilute cases as a result of the entrainment of background air.) Oxidation leads to

DOI: 10.1021/es506119x
Environ. Sci. Technol. 2015, 49, 4129−4137

an increase in f_S for upward (and slightly leftward) movement. A third process, deposition, also involves movement toward lower $[SO_2]$ and slightly higher f_S due to differences in SO_2 and sulfate deposition velocities.[34]

The extent of sulfate conversion is generally much greater at KMC than at Pahala. This indicates substantially more SO_2 oxidation under stagnant conditions as a result of differences in plume age and oxidation rate. The Pahala plume was intercepted only ∼5 h after emissions, whereas the emissions sampled at KMC could have been up to several days old because the stagnation event had begun a week earlier (on Jan. 12). However, age of the emissions cannot fully explain the differences in f_S in the two cases, because SO_2 reactivity also appears to vary. Even assuming an average age of 3 days (which is likely an upper limit), the f_S value of 0.3 would correspond to an average SO_2 oxidation rate of 1.4×10^{-6} s^{-1}, which is more than twice as fast as the rate on Feb. 3. Differences in oxidation rate in the two cases are even more pronounced if it is assumed that measured emissions are younger than this or if these inferred rates are compared against those from the other trade wind days (Feb. 4−6). This increased SO_2 reactivity at KMC suggests the presence of higher oxidant levels (in either the gas or droplet phase) in this stagnant case.

Particle Acidity and Neutralization. The sulfur-partitioning data in Figure 4 are colored according to particle acidity, with the color scale in each panel corresponding to a different acidity metric. Figure 4a shows the ammonium-to-sulfate ($[NH_4^+]/[SO_4^{2-}]$) ratio, as measured by the ACSM. Only ratios for which the absolute uncertainty is below 0.5 are shown; uncertainties were calculated from the scatter in the measurement of each aerosol component (1σ: 0.09 $\mu g/m^3$ for $[NH_4^+]$ and 0.08 $\mu g/m^3$ for $[SO_4^{2-}]$, based on clean-air measurements). The aerosol is only slightly neutralized by ammonia, with ratios mostly ranging from 0 (pure sulfuric acid) to 1 (ammonium bisulfate). Although aerosol mass spectrometry (AMS) measurements have previously found sulfate particles of volcanic origin to be acidic,[29−31] to our knowledge these measurements constitute the first AMS measurement of pure sulfuric acid particles in the ambient atmosphere. Levels of neutralization of the sulfate at Pahala are higher than at KMC, presumably as a result of terrestrial ammonia emissions encountered by the plume as it travels downwind over land, which includes agricultural areas. This is consistent with previous studies that also found increased ammonium levels in particles downwind of volcanic emissions.[19,20]

Data in Figure 4b are colored by aerosol pH (a measure of acidity within the particles), calculated using the Extended Aerosol Inorganics Model (E-AIM, model II: http://www.aim.env.uea.ac.uk/aim/aim.ph)[50] and assuming the only counterions are H^+ or NH_4^+. Inputs to the model are sulfate, ammonium, ambient relative humidity, and ambient temperature, and pH is determined from the calculated activity coefficients and concentrations of $[H^+]$. As in Figure 4a, only the pH values for data whose $[NH_4^+]/[SO_4^{2-}]$ ratios can be determined to within 0.5 are shown. The particles are highly acidic, ranging in pH from −0.8 (the equivalent of 6 M H_2SO_4) to 3.0. At such high acidity, the pH values actually do not correlate strongly with $[NH_4^+]/[SO_4^{2-}]$ because this ratio does not vary over a wide range. Instead, pH is mostly a function of ambient RH, with drier conditions (such as those encountered at Pahala) leading to less water uptake by the sulfate and, thus, higher H^+ activities within the particles.

Finally, the points in Figure 4c are colored by strong acidity (a measure of acidity per volume of air), determined from $2 \times [SO_4^{2-}] - [NH_4^+]$. Unlike the other two metrics of acidity ($[NH_4^+]/[SO_4^{2-}]$ and pH), strong acidity can be precisely determined even when $[NH_4^+]$ and $[SO_4^{2-}]$ are low, so values for all measurements are shown. Given the low level of neutralization of the particles, strong acidity depends largely on absolute sulfate levels, and so is poorly correlated with particle pH (which depends mostly on RH); thus, acidity normalized to the volume of air and acidity normalized to the volume of the particles are largely independent quantities in this case. Sulfate levels are highest during the stagnant days at KMC, leading to extremely high strong acidity values, of hundreds of $nmol/m^3$ when sampling aged emissions and up to 2200 $nmol/m^3$ when sampling fresh emissions. These values are far higher than those typically measured in ambient air, even under polluted urban conditions (where typical values are in the range of 50−200 $nmol/m^3$).[51,52]

Implications and Future Work. In general, measuring the chemistry and effects of individual emissions sources can be challenging because of complex and variable meteorology, uncertain chemical reactions, and interferences from other sources (background levels) of pollutants. However, the Kīlauea plume is in many ways an ideal system for measuring evolving plume chemistry: the prevailing meteorology is simple (enabling estimates of plume age), the key chemical transformations are relatively well-understood, and the point source is very intense and emits into clean air. These conditions, when coupled with highly time-resolved measurements of particle mass and chemical composition (as well as concentrations of the gas-phase precursor), allow for the detailed characterization of the factors controlling the formation and evolution of secondary particulate matter.

The real-time measurements made in this study show that the volcanic plume is highly variable and dynamic, and depends not only on emission rate and meteorology, but also on other factors that can vary strongly with location, time of day, and time of year. These include the daytime oxidant production (controlling SO_2 oxidation rate) as well as local emissions and relative humidity (controlling particle acidity). The effects of volcanic emissions on human and ecological health may thus also exhibit dependences on these factors; this is an important area of future research. Also important is the extension of these measurements to a wider range of locations and plume ages. In particular, time-resolved composition measurements at locations still further downwind will provide information on the role of plume chemistry over longer time scales as well as on the exposure of downwind communities to various components of the volcanic plume.

■ ASSOCIATED CONTENT

Supporting Information

Details of the ACSM operation and calibration, plus Figures S1−S4, showing (S1) a map of the Island of Hawai'i, with locations of volcanic vents and sampling sites; (S2) wind speed and direction at HVO and Pahala, showing differences in local meteorology at the two sites; (S3) cumulative probability distributions of SO_2 concentrations at Pahala; and (S4) a plot of sulfate mass concentration vs SO_2 concentration for all measurements. This material is available free of charge via the Internet at http://pubs.acs.org/.

DOI: 10.1021/es506119x
Environ. Sci. Technol. 2015, 49, 4129−4137

AUTHOR INFORMATION

Corresponding Author

*Phone: 617-253-2409; e-mail: jhkroll@mit.edu.

Author Contributions

[#]J.H.K. and E.S.C. contributed to this work equally.

Author Contributions

[‖]Members of TREX XII included Sara Comis, Brianna Coston, Flor De La Cruz, Michelle Dutt, Amairani Garcia, Majdolene Khweis, Elaine Kung, Matthew Monheit, Theresa Oehmke, Jessica Parker, Ricardo Ramos-Martin, Alexander Severt, and Phoebe Whitwell.

Author Contributions

[¶]Members of TREX XI included Jhanel Chew, Kelley Determan, Di Jin, Anna Kelly, Zara L'Heureux, Michelle Morales, Kelden Pehr, Marcela Rodriguez, Theresa Santiano-McHatton, Tara Soni, Priscilla Soto, Iovana Valdez, Jibo Wen, Jaclyn Wilson, Eric Alm, Kelly Daumit, Donald Frankel, and Janelle Thompson.

Notes

The authors declare no competing financial interest.

ACKNOWLEDGMENTS

Funding for this project was provided by MIT's Department of Civil and Environmental Engineering. We are grateful to the Hawai'i State Department of Health for access to their air quality monitoring station (Pahala measurements) and data and to the National Park Service for permitting research within Hawai'i Volcanoes National Park (KMC measurements, research permit HAVO-2012-SCI-0047) and for their online meteorological data. We also thank MIT's Sloan Engine Laboratory for use of their SO_2 monitor; Tamar Elias, Andrew J. Sutton, and Paul G. Okubo of the USGS Hawaiian Volcano Observatory for helpful advice, suggestions, and support; and Denise Miller for invaluable assistance with lodging and logistics.

REFERENCES

(1) Schmidt, A.; Carslaw, K. S.; Mann, G. W.; Rap, A.; Pringle, K. J.; Spracklen, D. V.; Wilson, M.; Forster, P. M. Importance of tropospheric volcanic aerosol for indirect radiative forcing of climate. *Atmos. Chem. Phys.* **2012**, *12*, 7321−7339.

(2) Andres, R. J.; Kasgnoc, A. D. A time-averaged inventory of subaerial volcanic sulfur emissions. *J. Geophys. Res. Atmos.* **1998**, *103*, 25251−25261.

(3) Allen, A. G.; Oppenheimer, C.; Ferm, M.; Baxter, P. J.; Horrocks, L. A.; Galle, B.; McGonigle, A. J. S.; Duffell, H. J. Primary sulfate aerosol and associated emissions from Masaya Volcano, Nicaragua. *J. Geophys. Res.* **2002**, *107*, ACH5−1−ACH5−8.

(4) IPCC. Climate Change 2013: The Physical Science Basis; Stocker, T. F., Qin, D., Plattner, G.-K., Tignor, M. M. B., Allen, S. K., Boschung, J., Nauels, A., Xia, Y., Bex, V., Midgely, P. M., Eds.; Cambridge University Press: Cambridge, UK, 2013; 1535 pp.

(5) Small, C.; Naumann, T. The global distribution of human population and recent volcanism. *Environ. Hazards* **2001**, *3*, 93−109.

(6) Hansell, A.; Oppenheimer, C. Health hazards from volcanic gases: A systematic literature review. *Arch. Environ. Health* **2004**, *59*, 628−639.

(7) Hansell, A. L. The health hazards of volcanoes and geothermal areas. *Occup. and Environ. Med.* **2006**, *63*, 149−156.

(8) Beirle, S.; Hörmann, C.; Penning de Vries, M.; Dörner, S.; Kern, C.; Wagner, T. Estimating the volcanic emission rate and atmospheric lifetime of SO_2 from space: A case study for Kīlauea volcano, Hawaii. *Atmos. Chem. Phys.* **2014**, *14*, 8309−8322.

(9) EPA. *The 2011 National Emissions Inventory*; version 1; United States Environmental Protection Agency: Washington, DC, 2012.

(10) Mannino, D. M.; Ruben, S. M.; Holschuh, F. C.; Holschuh, T. C.; Wilson, M. D.; Holschuh, T. Emergency department visits and hospitalizations for respiratory disease on the Island of Hawaii, 1981−1991. *Hawaii Med. J.* **1996**, *55*, 48−54.

(11) Longo, B. M.; Rossignol, A.; Green, J. B. Cardiorespiratory health effects associated with sulphurous volcanic air pollution. *Public Health* **2008**, *122*, 809−820.

(12) Longo, B. M.; Yang, W. Acute bronchitis and volcanic air pollution: A community-based cohort study at Kīlauea Volcano, Hawai'i, USA. *J. Toxicol. Environ. Health, Part A* **2008**, *71*, 1565−1571.

(13) Longo, B. M. The Kīlauea Volcano adult health study. *Nursing Res.* **2009**, *58*, 23−31.

(14) Longo, B. M.; Yang, W.; Green, J. B.; Crosby, F. L.; Crosby, V. L. Acute health effects associated with exposure to volcanic air pollution (vog) from increased activity at Kīlauea Volcano in 2008. *J. Toxicol. Environ. Health, Part A* **2010**, *73*, 1370−1381.

(15) Longo, B. M. Adverse health effects associated with increased activity at Kīlauea Volcano: A repeated population-based survey. *ISRN Public Health* **2013**, *2013*, 1−10.

(16) von Glasow, R. Atmospheric chemistry in volcanic plumes. *Proc. Natl. Acad. Sci. U.S.A.* **2010**, *107*, 6594−6599.

(17) von Glasow, R.; Bobrowski, N.; Kern, C. The effects of volcanic eruptions on atmospheric chemistry. *Chem. Geol.* **2009**, *263*, 131−142.

(18) McGonigle, A.; Delmelle, P.; Oppenheimer, C.; Tsanev, V. I.; Delfosse, T.; Williams-Jones, G.; Horton, K.; Mather, T. A. SO_2 depletion in tropospheric volcanic plumes. *Geophys. Res. Lett.* **2004**, *31*.

(19) Allen, A. G.; Baxter, P. J.; Ottley, C. J. Gas and particle emissions from Soufrière Hills Volcano, Montserrat, West Indies: Characterization and health hazard assessment. *Bull. Volcanol.* **2000**, *62*, 8−19.

(20) Mather, T. A.; Allen, A. G.; Oppenheimer, C.; Pyle, D. M.; McGonigle, A. J. S. Size-resolved characterisation of soluble ions in the particles in the tropospheric plume of Masaya Volcano, Nicaragua: Origins and plume processing. *J. Atmos Chem.* **2003**, *46*, 207−237.

(21) Oppenheimer, C.; Scaillet, B.; Martin, R. S. Sulfur degassing from volcanoes: Source conditions, surveillance, plume chemistry and Earth system impacts. *Rev. Mineral. Geochem.* **2011**, *73*, 363−421.

(22) Mather, T. A. Volcanism and the atmosphere: The potential role of the atmosphere in unlocking the reactivity of volcanic emissions. *Philos. Trans. R. Soc. A: Math., Phys. Eng. Sci.* **2008**, *366*, 4581−4595.

(23) Edmonds, M.; Sides, I. R.; Swanson, D. A.; Werner, C.; Martin, R. S.; Mather, T. A.; Herd, R. A.; Jones, R. L.; Mead, M. I.; Sawyer, G.; Roberts, T. J.; Sutton, A. J.; Elias, T. Magma storage, transport and degassing during the 2008−10 summit eruption at Kīlauea Volcano, Hawai'i. *Geochim. Cosmochim. Acta* **2013**, *123*, 284−301.

(24) Mather, T. A.; Witt, M. L. I.; Pyle, D. M.; Quayle, B. M.; Aiuppa, A.; Bagnato, E.; Martin, R. S.; Sims, K. W. W.; Edmonds, M.; Sutton, A. J.; Ilyinskaya, E. Halogens and trace metal emissions from the ongoing 2008 summit eruption of Kīlauea Volcano, Hawai'i. *Geochim. Cosmochim. Acta* **2012**, *83*, 292−323.

(25) Mather, T. A.; Tsanev, V. I.; Pyle, D. M.; McGonigle, A. J. S.; Oppenheimer, C.; Allen, A. G. Characterization and evolution of tropospheric plumes from Lascar and Villarrica Volcanoes, Chile. *J. Geophys. Res.* **2004**, *109*, D21303.

(26) Canagaratna, M. R.; Jayne, J. T.; Jimenez, J. L.; Allan, J. D.; Alfarra, M. R.; Zhang, Q.; Onasch, T. B.; Drewnick, F.; Coe, H.; Middlebrook, A.; Delia, A.; Williams, L. R.; Trimborn, A. M.; Northway, M. J.; DeCarlo, P. F.; Kolb, C. E.; Davidovits, P.; Worsnop, D. R. Chemical and microphysical characterization of ambient aerosols with the aerodyne aerosol mass spectrometer. *Mass Spectrom. Rev.* **2007**, *26*, 185−222.

(27) Ng, N. L.; Herndon, S. C.; Trimborn, A.; Canagaratna, M. R.; Croteau, P. L.; Onasch, T. B.; Sueper, D.; Worsnop, D. R.; Zhang, Q.; Sun, Y. L.; Jayne, J. T. An aerosol chemical speciation monitor (ACSM) for routine monitoring of the composition and mass concentrations of ambient aerosol. *Aerosol Sci. Technol.* **2011**, *45*, 780−794.

DOI: 10.1021/es506119x
Environ. Sci. Technol. 2015, 49, 4129−4137

(28) Carn, S. A.; Froyd, K. D.; Anderson, B. E.; Wennberg, P.; Crounse, J.; Spencer, K.; Dibb, J. E.; Krotkov, N. A.; Browell, E. V.; Hair, J. W.; Diskin, G.; Sachse, G.; Vay, S. A. In situ measurements of tropospheric volcanic plumes in Ecuador and Colombia during TC^4. *J. Geophys. Res.* **2011**, *116*, D00J24.
(29) DeCarlo, P. F.; Dunlea, E. J.; Kimmel, J. R.; Aiken, A. C.; Sueper, D.; Crounse, J.; Wennberg, P. O.; Emmons, L.; Shinozuka, Y.; Clarke, A.; Zhou, J.; Tomlinson, J.; Collins, D. R.; Knapp, D.; Weinheimer, A. J.; Montzka, D. D.; Campos, T.; Jimenez, J. C. Fast airborne aerosol size and chemistry measurements above Mexico City and Central Mexico during the MILAGRO campaign. *Atmos. Chem. Phys.* **2008**, *8*, 4027−4048.
(30) Ovadnevaite, J.; Ceburnis, D.; Plauskaite-Sukiene, K.; Modini, R.; Dupuy, R.; Rimselyte, I.; Ramonet, M.; Kvietkus, K.; Ristovski, Z.; Berresheim, H.; O'Dowd, C. D. Volcanic sulphate and arctic dust plumes over the North Atlantic Ocean. *Atmos. Environ.* **2009**, *43*, 4968−4974.
(31) O'Dowd, C.; Ceburnis, D.; Ovadnevaite, J.; Martucci, G.; Bialek, J.; Monahan, C.; Berresheim, H.; Vaishya, A.; Grigas, T.; Jennings, S. G.; McVeigh, P.; Varghese, S.; Flanagan, R.; Martin, D.; Moran, E.; Lambkin, K.; Semmier, T.; Perrino, C.; McGrath, R. The Eyjafjallajökull ash plume − Part I: Physical, chemical and optical characteristics. *Atmos. Environ.* **2012**, *48*, 129−142.
(32) Matthew, B. M.; Middlebrook, A. M.; Onasch, T. B. Collection efficiencies in an aerodyne aerosol mass spectrometer as a function of particle phase for laboratory generated aerosols. *Aerosol Sci. Technol.* **2008**, *42*, 884−898.
(33) Satsumabayashi, H.; Kawamura, M.; Katsuno, T.; Futaki, K.; Murano, K.; Carmichael, G. R.; Kajino, M.; Horiguchi, M.; Ueda, H. Effects of Miyake volcanic effluents on airborne particles and precipitation in central Japan. *J. Geophys. Res.* **2004**, *109*.
(34) Walcek, C. J.; Brost, R. A.; Chang, J. S.; Wesely, M. L. SO_2, sulfate and HNO_3 deposition velocities computed using regional landuse and meteorological data. *Atmos. Environ.* **1986**, *20*, 949−964.
(35) Harris, E.; Sinha, B.; van Pinxteren, D.; Tilgner, A.; Fomba, K. W.; Schneider, J.; Roth, A.; Gnauk, T.; Fahlbusch, B.; Mertes, S.; Lee, T.; Collett, J.; Foley, S.; Borrmann, S.; Hoppe, P.; Herrmann, H. Enhanced role of transition metal ion catalysis during in-cloud oxidation of SO_2. *Science* **2013**, *340*, 727−730.
(36) Welz, O.; Savee, J. D.; Osborn, D. L.; Vasu, S. S.; Percival, C. J.; Shallcross, D. E.; Taatjes, C. A. Direct kinetic measurements of Criegee intermediate (CH_2OO) formed by reaction of CH_2I with O_2. *Science* **2012**, *335*, 204−207.
(37) Hobbs, P. V.; Radke, L. F.; Lyons, J. H.; Ferek, R. J.; Coffman, D. J.; Casadevall, T. J. Airborne measurements of particle and gas emissions from the 1990 volcanic eruptions of Mount Redoubt. *J. Geophys. Res. Atmos.* **1991**, *96*, 18735−18752.
(38) Martin, R. S.; Sawyer, G. M.; Spampinato, L.; Salerno, G. G.; Ramirez, C.; Ilyinskaya, E.; Witt, M. L. I.; Mather, T. A.; Watson, I. M.; Phillips, J. C.; Oppenheimer, C. A total volatile inventory for Masaya Volcano, Nicaragua. *J. Geophys. Res.* **2010**, *115*, B09215.
(39) Saunders, S. M.; Jenkin, M. E.; Derwent, R. G.; Pilling, M. J. Protocol for the development of the Master Chemical Mechanism, MCM v3 (Part A): Tropospheric degradation of non-aromatic volatile organic compounds. *Atmos. Chem. Phys.* **2003**, *3*, 161−180.
(40) Atkinson, R.; Baulch, D. L.; Cox, R. A.; Crowley, J. N.; Hampson, R. F.; Hynes, R. G.; Jenkin, M. E.; Rossi, M. J.; Troe, J. Evaluated kinetic and photochemical data for atmospheric chemistry: Volume I − Gas phase reactions of O_x, HO_x, NO_x and SO_x species. *Atmos. Chem. Phys.* **2004**, *4*, 1461−1738.
(41) Stone, D.; Whalley, L. K.; Heard, D. E. Tropospheric OH and HO_2 radicals: Field measurements and model comparisons. *Chem. Soc. Rev.* **2012**, *41*, 6348.
(42) Hobbs, P. V.; Tuell, J. P.; Hegg, D. A.; Radke, L. F.; Eltgroth, M. W. Particles and gases in the emissions from the 1980−1981 volcanic eruptions of Mt. St. Helens. *J. Geophys. Res. Atmos.* **1982**, *87*, 11062−11086.
(43) Martin, D.; Ardouin, B.; Bergametti, G.; Carbonnelle, J.; Faivre Pierret, R.; Lambert, G.; Le Cloarec, M. F.; Sennequier, G. Geochemistry of sulfur in Mount Etna plume. *J. Geophys. Res. Atmos.* **2007**, *91*, 12249−12254.
(44) Krueger, A. J.; Schnetzler, C. C.; Walter, L. S. The December 1981 eruption of Nyamuragira volcano (Zaire), and the origin of the "mystery cloud" of early 1982. *J. Geophys. Res. Atmos.* **1996**, *101*, 15191−15196.
(45) Porter, J. N.; Horton, K. A.; Mouginis-Mark, P. J.; Lienert, B.; Sharma, S. K.; Lau, E.; Sutton, A. J.; Elias, T.; Oppenheimer, C. Sun photometer and lidar measurements of the plume from the Hawaii Kīlauea Volcano Pu'u O'o vent: Aerosol flux and SO_2 lifetime. *Geophys. Res. Lett.* **2002**, *29*, 30−1−30−4.
(46) Bluth, G. J. S.; Carn, S. A. Exceptional sulfur degassing from Nyamuragira Volcano. *International Journal of Remote Sensing* **2008**, *29* (22), 6667−6685.
(47) Rodríguez, L. A.; Watson, I. M.; Edmonds, M.; Ryan, G.; Hards, V.; Oppenheimer, C. M. M.; Bluth, G. J. S. SO_2 loss rates in the plume emitted by Soufrière Hills volcano, Montserrat. *J. Volcanol. Geotherm. Res.* **2008**, *173*, 135−147.
(48) McCormick, B. T.; Herzog, M.; Yang, J.; Edmonds, M.; Mather, T. A.; Carn, S. A.; Hidalgo, S.; Langmann, B. A comparison of satellite- and ground-based measurements of SO_2 emissions from Tungurahua Volcano, Ecuador. *J. Geophys. Res. Atmos.* **2014**, *119*, 4264−4285.
(49) Oppenheimer, C.; Francis, P.; Stix, J. Depletion rates of sulfur dioxide in tropospheric volcanic plumes. *Geophys. Res. Lett.* **1998**, *25*, 2671−2674.
(50) Clegg, S. L.; Brimblecombe, P.; Wexler, A. S. Thermodynamic model of the system H^+−NH_4^+−SO_4^{2-}−NO_3^-−H_2O at tropospheric temperatures. *J. Phys. Chem. A* **1998**, *102*, 2155−2171.
(51) Zhang, Q.; Jimenez, J. L.; Worsnop, D. R.; Canagaratna, M. A case study of urban particle acidity and its influence on secondary organic aerosol. *Environ. Sci. Technol.* **2007**, *41*, 3213−3219.
(52) Pathak, R. K.; Yao, X.; Lau, A. K. H.; Chan, C. K. Acidity and concentrations of ionic species of PM2.5 in Hong Kong. *Atmos. Environ.* **2003**, *37*, 1113−1124.

DOI: 10.1021/es506119x
Environ. Sci. Technol. 2015, 49, 4129−4137